Hindawi
Analytical Cellular Pathology
Volume 2023, Article ID 7940316, 14 pages
https://doi.org/10.1155/2023/7940316

Research Article

Association between CHFR and PARP-1, and Their Roles in Regulation of Proliferation and Apoptosis of B Cell Lymphoma

Xiao-Dan Liu,[1] Nian-Ju Zheng,[2] Liang Song,[1] Hua Pan,[1] and Ai-Qin Song[1]

[1]*Department of Pediatrics, The Affiliated Hospital of Qingdao University, Qingdao, Shandong 266000, China*
[2]*Department of Pediatrics, Jining Women and Children's Hospital, Jining, Shandong 272000, China*

Correspondence should be addressed to Ai-Qin Song; 18661807987@163.com

Received 7 June 2021; Revised 30 January 2023; Accepted 7 February 2023; Published 28 February 2023

Academic Editor: Consuelo Amantini

Background. Aberrant methylation of checkpoint with forkhead and ring finger domains (CHFR) was found in B-cell non-Hodgkin lymphoma (NHL), whereas its role in carcinogenesis is not clear. CHFR can control poly (ADP-ribose) polymerase levels by causing its degradation. The study was aimed to explore the roles and mechanisms of CHFR in the pathogenesis of B-cell NHL. *Methods*. Short hairpin ribonucleic acid (ShRNAs) targeting CHFR and poly (ADP-ribose) polymerase 1 (PARP-1) were transduced into Raji cells, and real-time polymerase chain reaction (PCR) and western blotting were carried out to determine their expression. Afterwards, the CCK-8 assay and flow cytometry were used to evaluate the cell growth and apoptosis. Tumor size and weight were determined using a xenograft model, and decitabine (5-Aza-dC) was used to further determine the methylation status of CHFR through a methylation specificity-PCR assay. *Results*. 5-Aza-dC-treatment promoted the expression of CHFR and decreased the expression of PARP-1 at both messenger ribonucleic acid (mRNA) and protein levels. 5-Aza-dC also accelerated Raji-cell apoptosis and restrained its growth *in vitro* and *in vivo* ($P < 0.05$). These results were contrary to those observed in the shRNA-CHFR group but consistent with those observed in the shRNA-PARP-1 group. The expression profiles of CHFR and PARP-1 in the xenograft model were consistent with those in the cellular model. Treatment with 5-Aza-dC led to demethylation of CHFR in nude mice. Besides, there may be a negative correlation between CHFR and PARP-1 in B-cell NHL cells. *Conclusion*. Our findings indicated that 5-Aza-dC could lead to the demethylation of the CHFR promoter and suppress Raji cell growth.

1. Introduction

Lymphoma is the most common malignancy during childhood and occurs in 16.6–23.2% of children with malignant tumors, second only to acute leukemia and intracranial tumors [1, 2]. Lymphoma tumors are classified into two groups, Hodgkin lymphoma (HL) and non-Hodgkin lymphoma (NHL). The latter has been widely studied because it accounts for 60% of malignant lymphomas, and often occurs in adolescents and adults with a poor prognosis and a higher chance of relapse. Recently, the incidence and mortality of B-cell NHL has increased despite treatments, such as high-dose chemotherapy and bone marrow transplantation. Because the alterations of genes and molecules contribute to the pathogenesis of cancers, it is essential to identify new potential targets for clinical targeted therapy.

Checkpoint with forkhead and ring finger domains (CHFR) is a mitotic checkpoint protein consisting of forkhead-associated (FHA), ring finger (RF), and cysteine-rich (CR) domains. FHA is a prerequisite for the mitotic checkpoint complex, and RF mediates the activity of E3 ubiquitin ligase. CHFR arrests cells in the pre-mitotic stage and enhances cell viability by disrupting chromosome condensation and centrosome separation via Cdc2/cyclin B. CHFR is reported to be widely expressed in human tissues. The expression of CHFR is frequently down-regulated in tumors, suggesting that CHFR may be a tumor suppressor gene [3]. Previous studies have shown that overexpression of CHFR could inhibit cell proliferation in HCT116 and RKO colon cancer cells, as well as in the Hs578T breast cancer cell line [4], indicating that CHFR may function as a negative regulator of proliferation, and may have anti-cancer

effects [5]. Additionally, poly (ADP-ribose) polymerase 1 (PARP-1) was identified as a novel CHFR-binding protein, and CHFR could regulate mitosis via the ubiquitylation and degradation of PARP-1 in a variety of cancer cells, including cervical cancer cells (HeLa), breast cancer cells (SK-BR-3 and ZR-75-1), gastric cancer cells (HSC-44, MKN7, and MKN45), non-small cell lung cancer cells (LU99), and colorectal cancer cells (HCT116 and DLD-1) [6]. The nuclear PARP-1 protein belongs to the poly (ADP-ribose) polymerase family, and has a DNA binding domain. PARP-1, an enzyme, can catalyze the covalent attachment of polymers of ADP-ribose (PAR) moieties on itself and its target proteins [7]. In addition, PARP-1 also plays an important role in DNA damage repair, cell cycle regulation, genome stability, and apoptosis [8–10]. PARP-1 was reported to be associated with the pathogenesis of tumors due to its up-regulation of expression and activity in many types of cancer [11, 12]. A study of Chung et al. [13] showed that Kaposi's sarcoma-associated herpesvirus (KSHV) down-regulated PARP-1 expression by PF-8 (a viral synthesis factor), and indicated that PF-8 could recruit host CHFR to target PARP-1 for proteasome degradation, thus promoting the efficient replication of KSHV cleavage. All these reports reveal the roles of PARP-1 in mitosis, and the interaction between CHFR and PARP-1 in cell cycle. However, the relationship between CHFR and PARP-1 is not clear in lymphoma.

Decitabine (5-Aza-dC) was approved for the treatment of myelodysplastic syndrome and leukemia by the Food and Drug Administration (FDA) in 2006 [14]. By covalently binding to methyltransferase, 5-Aza-dC leads to the demethylation and reactivation of the target gene. The abnormal hypermethylation of genes is widely detected in tumor tissues [15–17], which leads to the inactivation of tumor suppressor genes transcription [18]. It is proposed that CHFR loss may be caused by promoter CpG hypermethylation [19–22]. Accumulating evidence supports the role of the promoter hypermethylation-induced inactivation of CHFR in the pathogenesis of diverse tumors, including gastric cancer, non-small cell lung cancer, and colorectal cancer [21–23]. The status of expression and DNA methylation of CHFR in NHL is rarely reported.

Previously, CHFR was found to be decreased in NHL, suggesting that CHFR may be involved in the development of B-cell NHL [24, 25]. In the present study, CHFR was manipulated to be up-regulated in 5-Aza-dC-treated NHL Raji cells, and down-regulated using short hairpin ribonucleic acid (ShRNA) shRNA interference [26]. The purposes of this study were to explore the roles and mechanism of *CHFR* in the pathogenesis of NHL cells. These findings may support the use of CHFR and PARP-1 as potential therapeutic targets for lymphoma treatment.

2. Materials and Methods

2.1. Cell Culture. Human NHL Raji cells were purchased from the cell bank of the Chinese Academy of Sciences (Beijing, China), and maintained in RPMI 1640 medium supplemented with 10% fetal bovine serum (FBS) (Gibco, Grand Island, NY, USA), 100 kU/L penicillin, and 100 mg/L streptomycin in a CO_2 thermostat at 37°C.

2.2. Experimental Group. Based on previous results [24], Raji cells were treated with phosphate buffered saline (PBS) as a blank control or 5-Aza-dC. After that, for lentivirus particle transfection, the Raji cells were divided into shRNA-CHFR, blank, and negative control (NC) groups; or shRNA-PARP-1, blank, and NC groups. At least three replicates were included in each group.

2.3. 5-Aza-dC Treatment and Lentivirus Transfection. Raji cells were seeded into the culture flask, and then treated with 5-Aza-dC (10 μmol/L) for 24 hours. An equal amount of PBS was used as blank control. The cells were then harvested after 24 hour for further analysis.

shRNA vectors, including shRNA-CHFR, shRNA-PARP-1, and NC, were constructed by Shanghai GeneChem Co., Ltd. (Shanghai, China). The sequences were shown as follows: shRNA-CHFR 5′-GTCAGACATCCTGAAGAAT-3′, NC 5′-TTCTCCGAACGTGTCACGT-3′; shRNA-PARP-1 5′-GATAGAGCGTGAAGGCGAA-3′, and NC 5′-TTCTCCGAACGTGTCACGT-3′. Based on the previous study [27], the lentivirus transfection was conducted. Briefly, Raji cells (5×10^4/well) were seeded into 96-well plates, and then transfected with lentivirus particles at 3×10^8 TU/mL using Lipofectamine 2000 (Thermo Fisher Scientific, Waltham, MA, USA) in accordance with the manufacturer's instructions. The different lentivirus particles were shown as follows: in the NC group, 100 μL culture media in the blank group, 90 μL culture media + 10 μL NC lentivirus; as well as in the shRNA-CHFR or shRNA-PARP-1 group, 100 μL shRNA-CHFR or shRNA-PARP-1 lentivirus + 800 μL ENI.S + P(E) containing 500 μg/mL polybrene. At 24, 48, and 72 hours of post-transfection, cell viability and transfection rate were measured. Success was defined as an infection rate (fluorescence intensity) >80%.

2.4. Real-Time Quantification Polymerase Chain Reaction. Raji cells or tumor tissues were harvested, and then lysed with TRIzol (Takara, Osaka City, Osaka Prefecture, Japan) according to the manufacturer's instructions. Total RNAs were reverse-transcribed into complementary DNA (cDNA), and real-time quantification polymerase chain reaction (RT-qPCR) was performed using LightCycler 96 Real-Time PCR System using the following primers synthesized by Sangon Biotech (Shanghai) Co., Ltd. (Shanghai, China): CHFR forward 5′-CCTCAACAACCTCGTGGAAGCATAC-3′ and reverse 5′-TCCTGGCATCCATACTTTGCACAT-3′; PARP-1 forward 5′-GTGTGGGAAGACCAAAGGAA-3′ and reverse 5′-TTCAAGAGCTCCCATGTTCA-3′; and β-actin forward 5′-AGCTACGAGCTGCCTGAC-3′ and reverse 5′-AAGGTA GTTTCGTGGATGC-3′. The relative expression of targeted genes was determined using the $2^{-\Delta\Delta Ct}$ method.

2.5. Western Blotting. Raji cells with different treatments were harvested and lysed in a lysis buffer. The protein expression of CHFR and PARP-1 was determined using western blotting as previously described [28, 29]. Briefly,

the obtained protein samples (20 μg) were separated by sodium dodecyl sulfate polyacrylamide gel electrophoresis (SDS–PAGE) and transferred to polyvinylidene fluoride (PVDF) membranes. Afterwards, the PVDF membranes were blocked with 5% skim milk at room temperature for 1 hour, and then incubated with the primary antibody against CHFR (1 : 1500, Cell Signaling Technology, Boston, MA, USA) and PARP-1 (1 : 1500, Abcam, Boston, MA, USA) at 4°C, overnight. After washing thrice in TBS (Tris-HCL) + Tween (TBST), the membranes were incubated with the secondary anti-mouse or anti-rabbit antibody (1 : 2000, Abcam, Boston, MA, USA) for 2 hours at 37°C. Finally, the protein bands were visualized using an ECL kit (Amersham Biosciences Co., Washington, WA, USA).

2.6. Cell Viability Assay. According to the manufacturer's protocol (Boster Biological Tech, Wuhan, China), the ability of cell proliferation was measured using Cell Counting Kit-8 (CCK-8, Beyotime Biotechnology, Shanghai, China). In brief, 100 μL cells in the blank, NC, and sh-CHFR or shRNA-PARP-1 groups (1.0×10^5/mL) were seeded onto 96-well plates and cultured for 24 and 48 hours at 37°C. Then, 10 μL CCK-8 was added to each well and the mixed samples were incubated for 24 and 48 hours. The inhibitory rate was calculated using the equation: 1 − (OD450 exp − OD450 blank)/(OD450 con − OD450 blank), where 'exp' indicates cells overexpressing or down-regulating targeted genes.

2.7. Cell Apoptosis Assay. The cell apoptosis of Raji cells was determined using Annexin V-FITC cell apoptosis assay kit (Beyotime Biotechnology) following the recommendations of the manufacturer. 1×10^6 Raji cells with different treatments (blank, NC, and sh-CHFR or shRNA-PARP-1 groups) were collected in a centrifuge tube (10 mL), and centrifuged at 1000 rpm for 5 minutes. After washing with PBS, the cells were centrifuged again, and labelled with 5 μL Annexin V and 5 μL 7AAD (BD Biosciences, Franklin Lake, NJ, USA) for 5 minutes in the dark. Apoptotic cells were detected using a flow cytometer (BD Biosciences).

2.8. Tumor Xenograft Model. When Raji cells grew to the logarithmic phase, the cells were treated with PBS or 5-Aza-dC, or transfected with shRNA-CHFR or shRNA-PARP-1 or shRNA-NC for 48 hours. After that, the cells with different treatments were harvested, and then counted the viable cells in each group. After that, the cell suspension was adjusted to 3×10^7 cells/mL with serum-free medium.

A total of 20 four-to-six-week-old male nude mice were divided into five groups using a random number table method ($n = 4$): blank group, 5-Aza-Dc group, shRNA-CHFR group, shRNA-PARP-1 group, and shRNA-NC group. The mice in the 5-Aza-dC group, shRNA-CHFR group, shRNA-PARP-1, and shRNA-NC group were, respectively, subcutaneously injected with cell suspension (200 μL) treated with 5-Aza-dC and transfected with shRNA-CHFR or shRNA-PARP-1 or shRNA-NC for 48 hours to the right subaxillary, once every two days for five times. The mice in the blank group were injected with the cell suspension that was treated with PBS. At day 10, the tumor xenograft model was defined to be successful if the short diameter was 0.42 cm [30]. The tumor volumes and body weights of all the mice were dynamically monitored. The following equation was used to calculate the tumor volume:

$$\text{Tumor volume} = a \times b^2/2, \quad (1)$$

where a represents the longer diameter of the tumor and b represents the shorter diameter of the tumor.

At day 24, all the mice were sacrificed by cervical dislocation method, and the tumor weight and volume were recorded. At the same time, all the nude mice were dissected to observe whether there were metastases, such as lung nodules, visible to the naked eye. The obtained tumor tissues were stored at −80°C for subsequent experiments. All the animal experiments were in line with the ARRIVE guidelines and the animal ethics committee of The Affiliated Hospital of Qingdao University, Qingdao, China.

2.9. Detection of Cell Apoptosis and Tumor Microvascular Density In Vivo. The tumor tissues in the different groups were collected for cell apoptosis using Terminal Deoxynucleotidyl Transferase mediated dUTP Nick-End Labeling (TUNEL). The tumor tissues were fixed, embedded in paraffin, and then cut into 5-μm sections. After that, the tumor sections were dewaxed, dehydrated by gradient ethanol, digested by 20 g/L protease K at room temperature, and then stained by TUNEL method. After sealed with neutral resin, the images were observed under a microscope at 200× magnification. The presence of brown reagent in the nucleus was considered as positive, and the presence of blue nucleus was considered as negative. The negative and positive controls were set at the same time. At least three visual fields were counted in each section, and then the cell apoptosis rate was calculated.

The tumor microvascular density in the different groups was assessed by immunohistochemistry of CD34. The tumor sections were dewaxed, dehydrated by gradient ethanol, and incubated in BSA for 30 minutes after antigen repair. Afterwards, the samples were incubated with anti-CD34 antibody, and then incubated with the secondary antibody. After 3,3'-diaminobenzidine (DAB) staining and hematoxylin contrast staining, the samples were sealed with neutral resin, and the pictures were found under a microscope at 200× magnification. Three areas with the highest blood vessel density were determined in each section under low power lens, and then the number of microvessels in each area was counted under high power lens, and the values of microvascular density were calculated. The negative and positive controls were set at the same time.

2.10. Determination of Methylation. Total DNA from tumor tissues and Raji cells in the different groups was extracted using a DNA extraction kit (Promega, Madison, WI, USA) following the manufacturer's protocols, and then were modified with sodium hydrogen sulfite. The sequences of the

modified primers were displayed as follows: CHFR methylated (CHFR-M) primer, forward 5′-TTTCGT-GATTCG TAGGCGAC-3′ and reverse 5′-GCGATTAACTAAC-GACGACG-3′. CHFR unmethylated (CHFR-U) primer, forward 5′-TTTTGTGATTTGTAGGTGAT-3′ and reverse 5′-ACAATTAACTAACAACAACA-3′. The methylation of CHFR was determined by methylation specificity-PCR (MSP). The MSP reaction was initiated at 95°C for 5 minutes, followed by a total cycle of 45 at 95°C for 30 seconds, 58°C (methylation)/53°C (unmethylation) for 30 seconds, and 72°C for 45 seconds. The MSP product (3 μL) was then used for 1.5% agarose gel electrophoresis (110 mV), and the results were analyzed based on the bands.

2.11. Statistical Analysis. All the data in this study were expressed as mean ± SD ($\bar{X} \pm S$) and analyzed using SPSS20. Differences between two groups were analyzed by *t*-test, and differences among multiple groups were calculated using one-way Analysis of Variance (ANOVA). $P < 0.05$ was considered statistically significant.

3. Results

3.1. Lentivirus-Mediated Transfection of CHFR and PARP. In order to screen the optimal multiplicity of infection (MOI), the Raji cells were transfected with different MOI of sh-CHFR and sh-PARP lentivirus for 72 hours, and the fluorescence intensity was determined. At 72 hours post-infection, the fluorescence intensity of these cells gradually increased along with the MOI values (Figure 1(a)). A MOI value of 30 was decided to be optimal given the virus titers and cytotoxicity. Moreover, we detected a stronger Green fluorescent protein (GFP) intensity at 72 hours post-infection, with an infection rate >80%. The cells after transfection were observed under a light microscope (Figure 1(b)). Additionally, there was no significant difference in the cell viability among the control cells and the cells transfected with different MOI of shRNA NC after cultured for 24, 48, and 72 hours ($P > 0.05$; Figure 1(c)). This indicated that shRNA NC lentivirus packaging did not significantly affect the viability of Raji cells. Therefore, we chose the MOI value of 30 for further cell transfection.

3.2. The Effect of 5-Aza-dC on Expression Levels of CHFR and PARP-1 in Raji Cells. In order to see the effects of 5-Aza-dC on the expression levels of CHFR and PARP-1 in Raji cells, the cells were treated with 5-Aza-dC (10 μmol/L) for 24 hours, and then RT-qPCR and western blotting were performed. Compared with the control group, the expression level of *CHFR* was significantly increased ($P < 0.05$), whereas the expression level of *PARP-1* was significantly decreased ($P < 0.05$; Figure 2(a)). Additionally, the change tendency of CHFR and PARP-1 detected by western blotting was similar to that measured by RT-qPCR (Figure 2(b)). These results indicated that 5-Aza-dC could upregulate the expression of CHFR and down-regulate the expression of PARP-1.

After that, the methylation of CHFR in the Raji cells was measured. After being amplified with methylated or unmethylated primers, there were no bands in the blank control group (only the medium, lane 7 and 8). However, in the positive control group (the normal peripheral blood treated with Sssl methyl transferase, lane 5 and 6), and the control group (the Raji cells with PBS, lane 3 and 4), the bands were observed after amplification with the methylated primers (lane 5 and 3), which indicated that *CHFR* was methylated in the Raji cells. After the Raji cells treated with 5-Aza-dC, the bands (lane 1 and 2) were both visualized after amplification with the methylated and unmethylated primers, as well as compared with the control group (lane 3), the band after amplification with methylated primers in the treatment group (lane 1) was weaker and lighter, which implied that 5-Aza-dC could partially demethylate *CHFR* in the Raji cells (Figure 2(c)).

3.3. The Expression Levels of CHFR and PARP-1 after Cell Transfection. Raji cells were transfected with NC sh sequences, sh-CHFR, or sh-PARP lentivirus for 48 hours, and then the expression levels of CHFR and PARP-1 were determined using RT-qPCR and western blot. The cells in the blank group were without treatment. It is obvious that there were no significant differences in the mRNA expression levels of *CHRF* and *PARP-1* between the blank group and NC group ($P > 0.05$; Figures 3(a) and 3(b)). Compared with the blank group, the expression level of *CHFR* was significantly decreased in the ShRNA-CHFR group ($P < 0.05$), whereas the expression level of *PARP-1* was significantly increased in the ShRNA-CHFR group ($P < 0.05$; Figure 3(a)). However, after *PARP-1* silencing, the expression level of *CHFR* was evidently increased in the ShRNA-PARP-1, and the expression level of *PARP-1* was decreased ($P < 0.05$; Figure 3(b)). Additionally, western blotting showed the similar trends after *CHFR* or *PARP-1* silencing (Figures 3(c) and 3(d)). These results suggested that silencing *CHFR* could reduce the expression level of CHFR, and increase the expression level of PARP-1, whereas silencing PARP-1 could promote the expression level of CHFR, and inhibit the expression level of PARP-1.

3.4. The Effects of CHFR and PARP-1 on Cell Viability and Apoptosis of Raji Cells. Further to investigate the effects of *CHFR* and *PARP-1* on the growth of Raji cells, the Raji cells with CHFR/PARP-1 knockdown were established using lentivirus packaging, and then cultured for 24 and 48 hours. The cells in the blank group were without treatment. After that, CCK-8 kit and flow cytometer were used to determine their viability and apoptosis. It is obvious that there was no significant difference in the cell viability of Raji cells between the blank group and NC group ($P > 0.05$; Figure 4). The cell viability was significantly higher in the ShRNA-CHFR group than that in the blank group cultured for 24 or 48 hours ($P < 0.05$; Figure 4(a)). However, after silencing *PARP-1*, the cell viability of Raji cells was evidently inhibited compared with the blank group ($P < 0.05$; Figure 4(b)).

In addition, no significant differences in the cell apoptosis of Raji cells between the blank groups and their corresponding NC groups in the experiments of silencing *CHFR* or *PARP-1* were found ($P > 0.05$; Figure 5). The cell apoptosis rates in the blank group and the shRNA-CHFR group were 15.61 ± 0.24% and 9.21 ± 0.53%, respectively, which

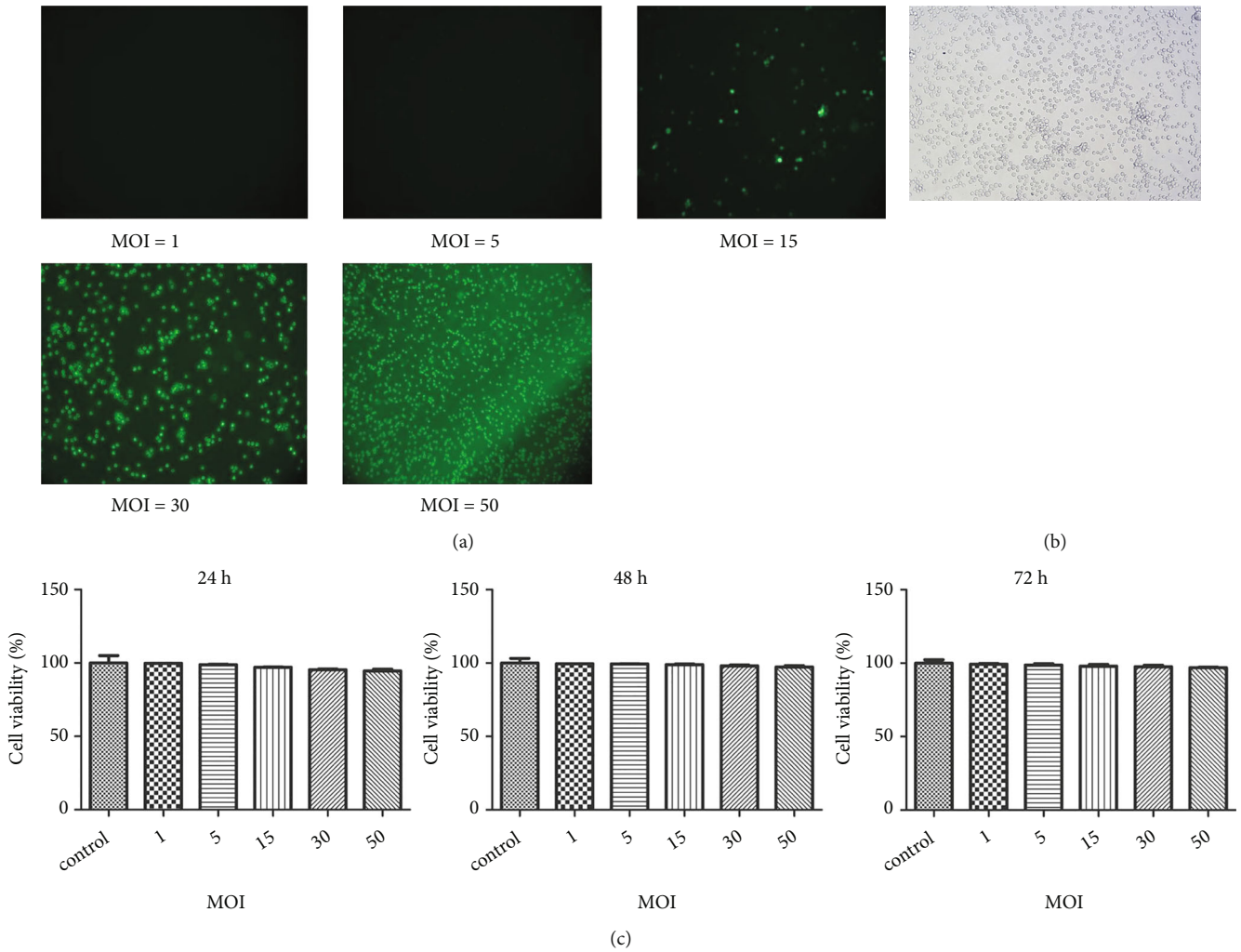

Figure 1: Lentivirus-mediated transfection efficiency after 72 hours post-infection. (a) Fluorescence intensity in Raji cells after transfection with different MOI for 72 hours under a fluorescence microscope. (b) The cellular morphology after transfection for 72 hours under a light microscope. (c) The cell viability of the cells transfected with different MOI of shRNA negative control (NC) after cultured for 24, 48, and 72 hours using cell counting kit-8.

showed a significant decrease after silencing *CHFR* ($P < 0.05$; Figure 5(a)). However, a significant increase of cell apoptosis rate was observed in the shRNA-PARP-1 group ($37 \pm 0.93\%$) compared with the corresponding blank group ($11.4 \pm 0.90\%$, $P < 0.05$; Figure 5(b)). Taken together, CHFR knockdown could promote the viability of Raji cells, and inhibit their apoptosis; whereas the effects of PARP-1 knockdown on Raji cells were opposite to CHFR knockdown.

3.5. The Role of CHFR Promotor Methylation in Tumor Xenograft Mice In Vivo. To further explore the roles of CHFR and PARP-1 *in vivo*, the nude mice were injected with the suspension of cells previously treated with different treatments at 6×10^6 cells/time. After fed for 24 days, the tumor size and volume of all mice were measured and recorded. Small visible tumors were observed at one week after the subcutaneous injection of Raji cells. The shorter diameter reached to 0.4 cm two weeks later, and the tumor size was gradually increased in a time-dependent manner (Figures 6(a), 6(b), and 6(c)). At day 24, it is obvious that the tumor volume or weight was significantly lower in the 5-Aza-dc and ShRNA-PARP-1 groups than that in the blank group ($P < 0.05$), whereas it was significantly higher in the ShRNA-CHFR group ($P < 0.05$; Figure 6(d)). No significant differences were found in the tumor volume/weight, cell apoptosis rate, and tumor microvascular density between the blank and ShRNA-NC groups ($P > 0.05$; Figures 6(d), 6(e), and 6(f)). Compared with the blank group, the cell apoptosis rate was significantly increased in the 5-Aza-dc and ShRNA-PARP-1 groups ($P < 0.05$); whereas was significantly reduced in the ShRNA-CHFR group ($P < 0.05$; Figure 6(e)). The tendency of the tumor microvascular density in the different groups was opposite to that of the cell apoptosis rate (Figure 6(f)).

Additionally, there were no significant differences in the expression of CHFR and PARP-1 between the blank and ShRNA-NC groups ($P > 0.05$; Figure 6(g)). Compared with the blank group, the *CHFR* expression was significantly up-

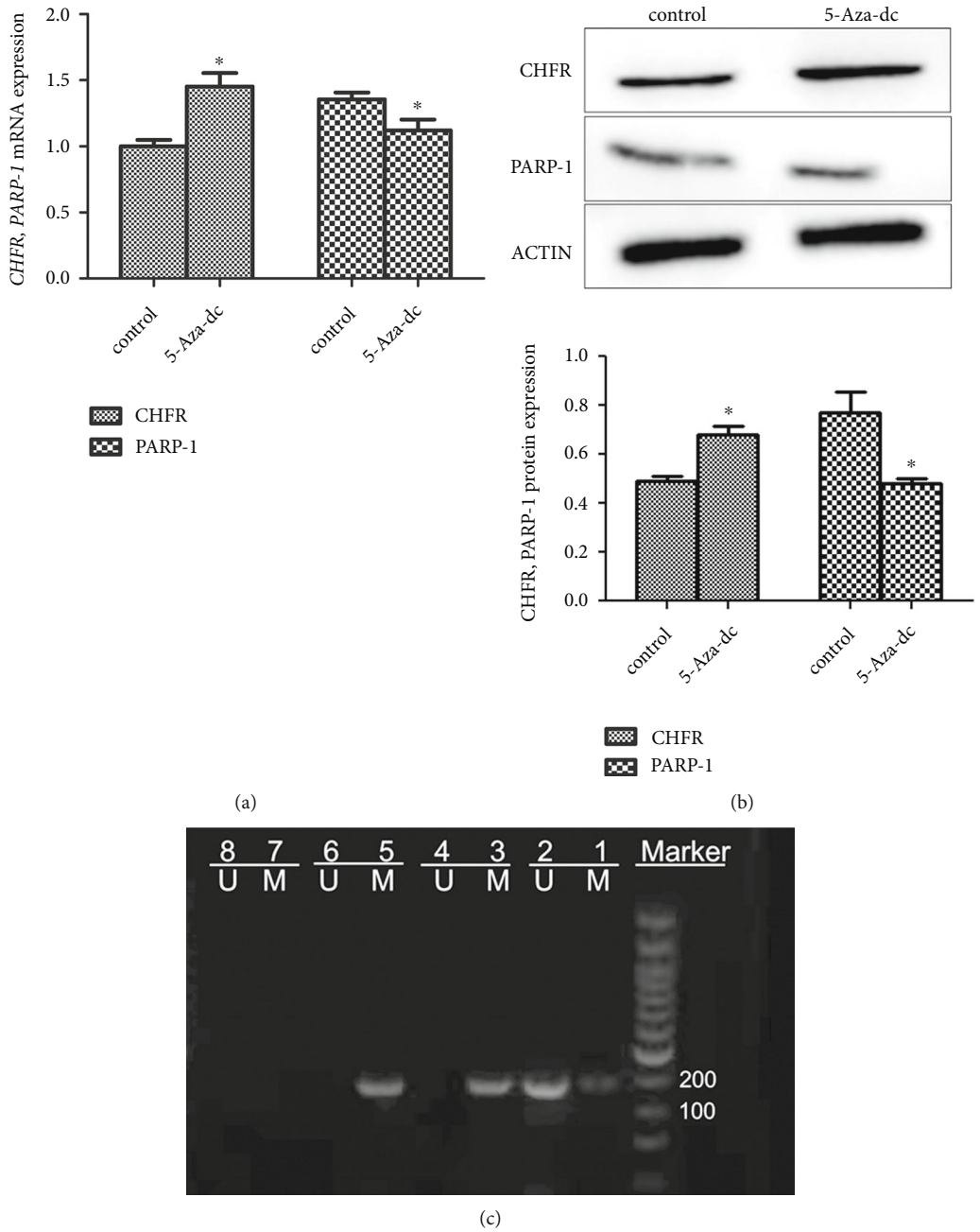

Figure 2: The effects of 5-Aza-dc on the expression levels of CHFR and PARP-1, as well as CHFR methylation in Raji cells. (a) The mRNA expression levels of *PARP-1* and *CHFR* in the cells treated with 5-Aza-dc for 24 hours determined by real-time quantification PCR (RT-qPCR). (b) The protein expression levels of PARP-1 and CHFR in the cells treated with 5-Aza-dc for 24 hours measured by western blotting. (c) The methylation of CHFR in Raji cells using methylation specificity-PCR (MSP; M: methylation; U: unmethylation; 1, 2: treatment group, the Raji cells treated with 5-Aza-dC; 3, 4: control group, the Raji cells treated with PBS; 5, 6: positive control group, the normal peripheral blood treated with SssI methyl transferase; 7, 8: blank control group, only the medium). $^{*}P < 0.05$, compared with the control group.

regulated in the 5-Aza-dC and ShRNA-PARP-1 groups; whereas it was obviously down-regulated in the ShRNA-CHFR group ($P < 0.05$; Figure 6(g)). However, the trend of *PARP-1* expression level was opposite to that of *CHFR* expression (Figure 6(g)). Besides, CHFR methylation was then determined in the tumor tissues using MSP. The results of CHFR in the tumor tissues were similar to those in the Raji cells (Figure 6(h)). No bands (lane 7 and 8) were observed in the blank control (the normal mice), as well as the bands (lane 5 and 3) were found in the control group (the Raji cells-induced mice injected with PBS) and positive control group (the normal peripheral blood treated with Sssl methyl transferase) after amplification with the methylated primers. After the Raji cells-induced mice treated with 5-Aza-dC treatment, the bands (lane 1 and 2) were observed after amplification with the methylated and unmethylated primers, and the band

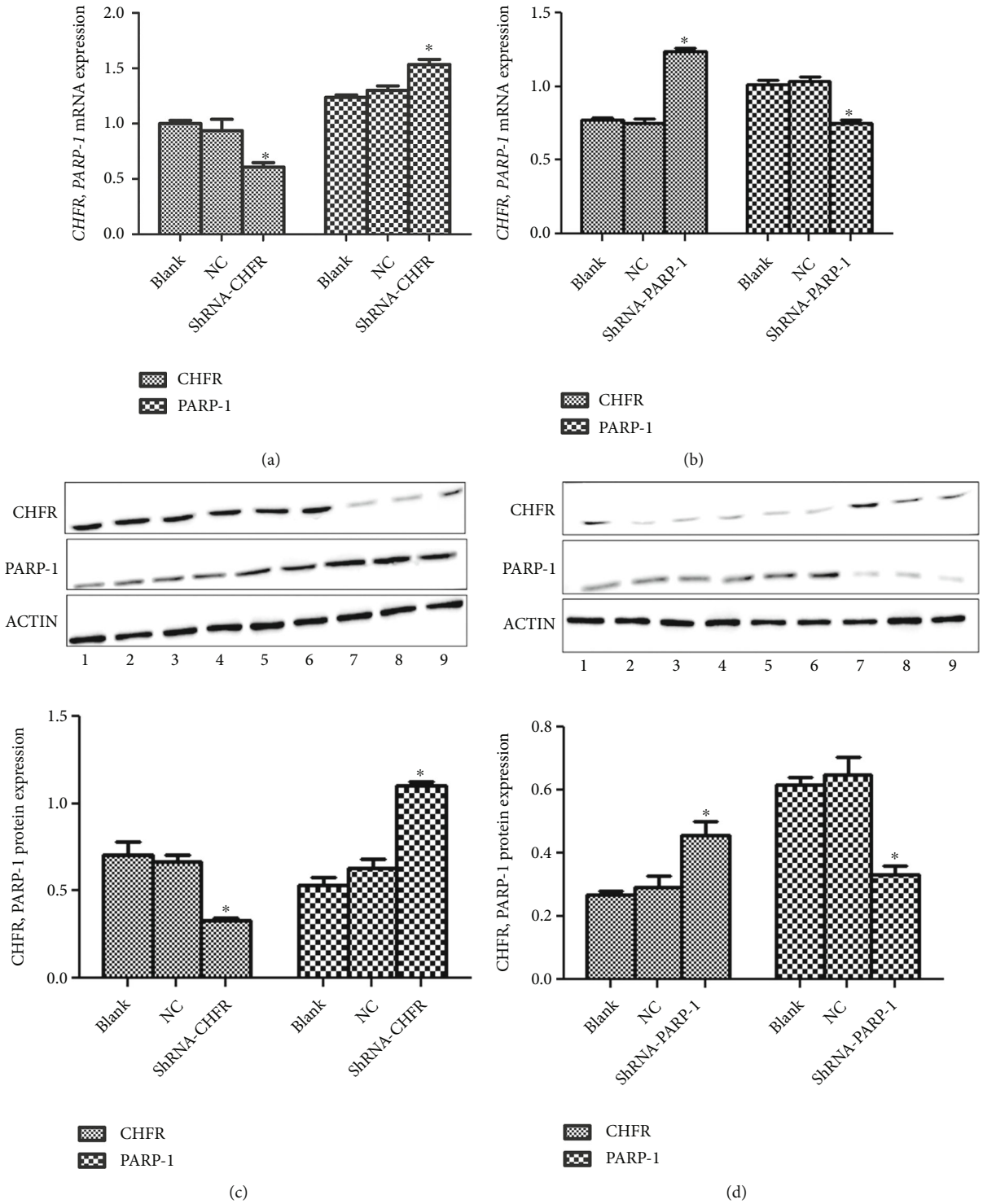

Figure 3: The cell transfection efficiency after the cells' transfection with negative control (NC), sh-CHFR, and sh-PARP-1 lentivirus for 48 hours was evaluated by determining the expression of CHFR and PARP-1. The mRNA expression levels of *CHFR* and *PARP-1* after CHFR interference (a) and PARP-1 interference (b) determined by RT-qPCR. The protein expression levels of CHFR and PARP-1 after CHFR interference (c) and PARP-1 interference (d) measured by western blotting. 1–3: the cells without treatment (blank group); 4–6: the cells transfected with NC (NC group); 7–9: the cells transfected with sh-CHFR or sh-PARP-1 lentivirus (transfection group). $^{*}P < 0.05$, compared with the blank group.

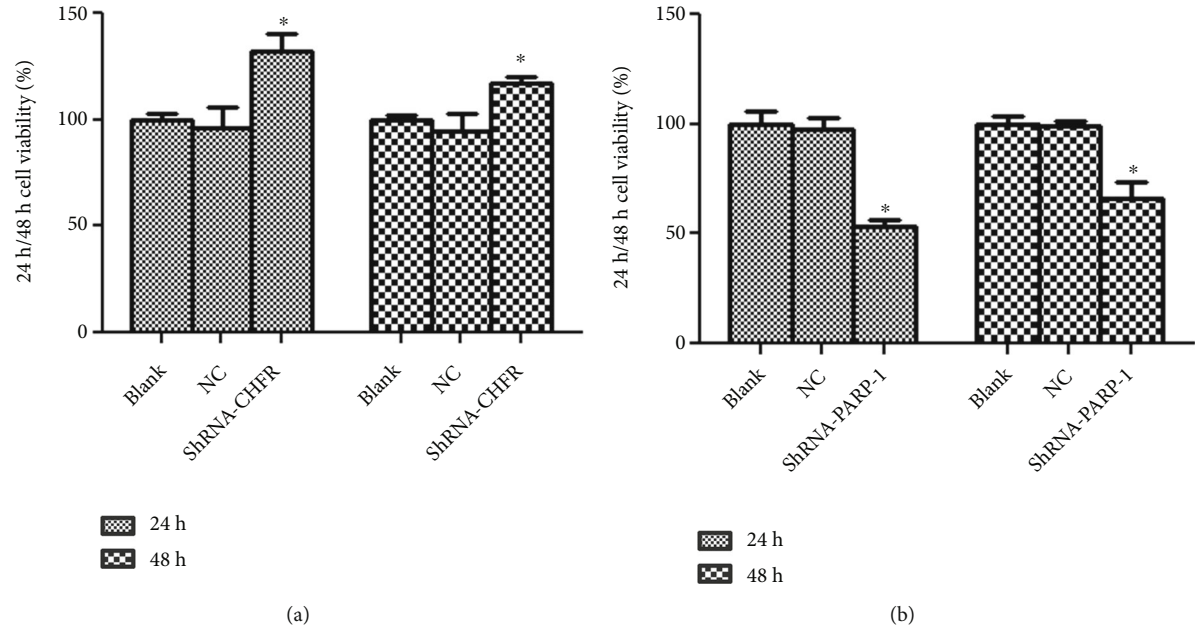

Figure 4: The effects of CHFR and PARP-1 on the cell viability of Raji cells using cell counting kit-8. The relative cell viability of Raji cells after the cells' transfection with sh-CHFR (a) and sh-PARP-1 (b) lentivirus for 24 and 48 hours determined by cell counting kit-8. $^*P < 0.05$, compared with the blank group.

(lane 1) was weaker compared with the control group (Figure 6(h)). These implied that 5-Aza-dC could demethylate *CHFR* in transplanted tumor tissues (Figure 6(h)).

4. Discussion

CHFR, a gene of mitotic checkpoint, regulates a delay of mitotic stress at G2/M phase [25], and controls both a new prophase checkpoints early in mitosis and chromosome segregation later in mitosis to maintain genomic stability [31]. PARP-1 is the most abundant and founding member of the PARP family, and its high expression is detected in various tumors, including breast, ovarian, bladder, colorectal, and gastric cancers [32–35], as well as NHL Raji cells [35]. A recent study reported that in CHFR-expressing cells, mitotic stress induced the autoPARylation of PARP-1, leading to an enhanced interaction between CHFR and PARP-1, and increase in the polyubiquitination/degradation of PARP-1, which implied that the interaction between CHFR and PARP-1 plays an important role in cell cycle regulation and cancer therapeutic strategies [6]. Besides, PARP-1 expression is significantly higher in malignant lymphoma compared with normal lymph nodes [36], and down-regulation of PARP-1 inhibits the cells in the G2/M phase [6]. Our study further investigated the relationships between CHFR and PARP-1 *in vitro* and *in vivo* in NHL.

PAR-binding zinc-finger (PBZ) domain is a receptor of PARPs in the CR region of CHFR, and mutations in the PBZ domain contribute to a loss of CHFR's mitotic checkpoint function [37, 38]. Evidences have shown that G2/M arrest is prolonged in PARP-1-deficient cells, and PARP-1 and PARylation play essential roles in cell entrance into mitosis, chromosomal aggregation, and cell division [39–41]. In the mitotic stress condition, the reduction in PARP-1 protein levels has been reported to lead to prophase cell cycle arrest, and CHFR can function in cell cycle arrest by lowering PARP-1 levels before entering mitosis where adequate PARP-1 will be required [6]. A previous study of Kashima et al. [8] also showed that CHFR can control PARP levels by causing its degradation, but that was in the conditions of mitotic stress and cell arrest, caused by this mechanism, and in fact led to increased cell survival. However, in this study, PARP-1 expression was significantly up-regulated in the *CHFR* knocked down Raji cells; as well as CHFR expression was also significantly up-regulated in the shRNA-PARP-1 Raji cells. These data suggested CHFR and PARP-1 had a crosstalk in the normal condition, and there may be a negative correlation between CHFR and PARP-1 in NHL Raji cells. Combined with our results, we speculate that CHFR interacts with PARP-1 not only under stress or damaged conditions, but also possibly under normal conditions.

Furthermore, we explored the roles of CHFR and PARP-1 in NHL *in vivo* and *in vitro*. Both *in vitro* and *in vivo* experiments showed that *CHFR* knockdown could enhance Raji cell viability, suppress cell apoptosis, and promote tumor formation; whereas silencing *PARP-1* could inhibit Raji cell viability and tumor growth, and induce Raji cell apoptosis. PARP-1 initiates a variety of cellular responses, including DNA repair, cell cycle checkpoint control, apoptosis, and transcription in the nucleus [6]; as well as dysregulation of PARP-1 is closely associated with the DNA damage and tumor development [42, 43]. CHFR can recognize the PARylation signals at the sites of DNA damage, and the loss of CHFR can prolong the retention time of PARP-1 at damage sites, which may inhibit DNA damage repair and induce the accumulation of DNA damage [43, 44]. Lacking

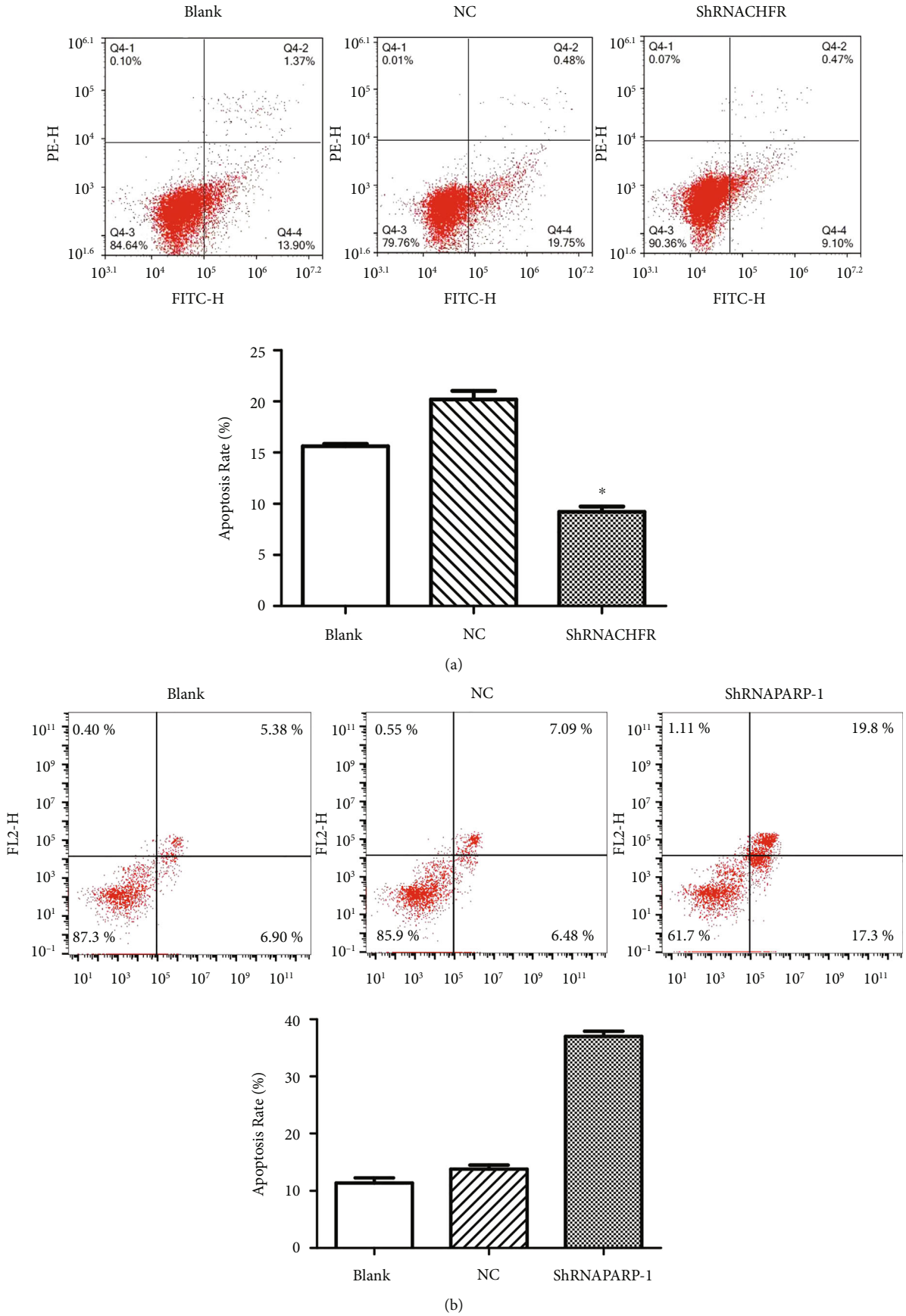

Figure 5: The effects of CHFR and PARP-1 on the cell apoptosis of Raji cells. The cell apoptosis of Raji cells after the cells' transfection with sh-CHFR (a) and sh-PARP-1 (b) lentivirus for 24 and 48 hours measured using flow cytometry. $^{*}P < 0.05$, compared with the blank group.

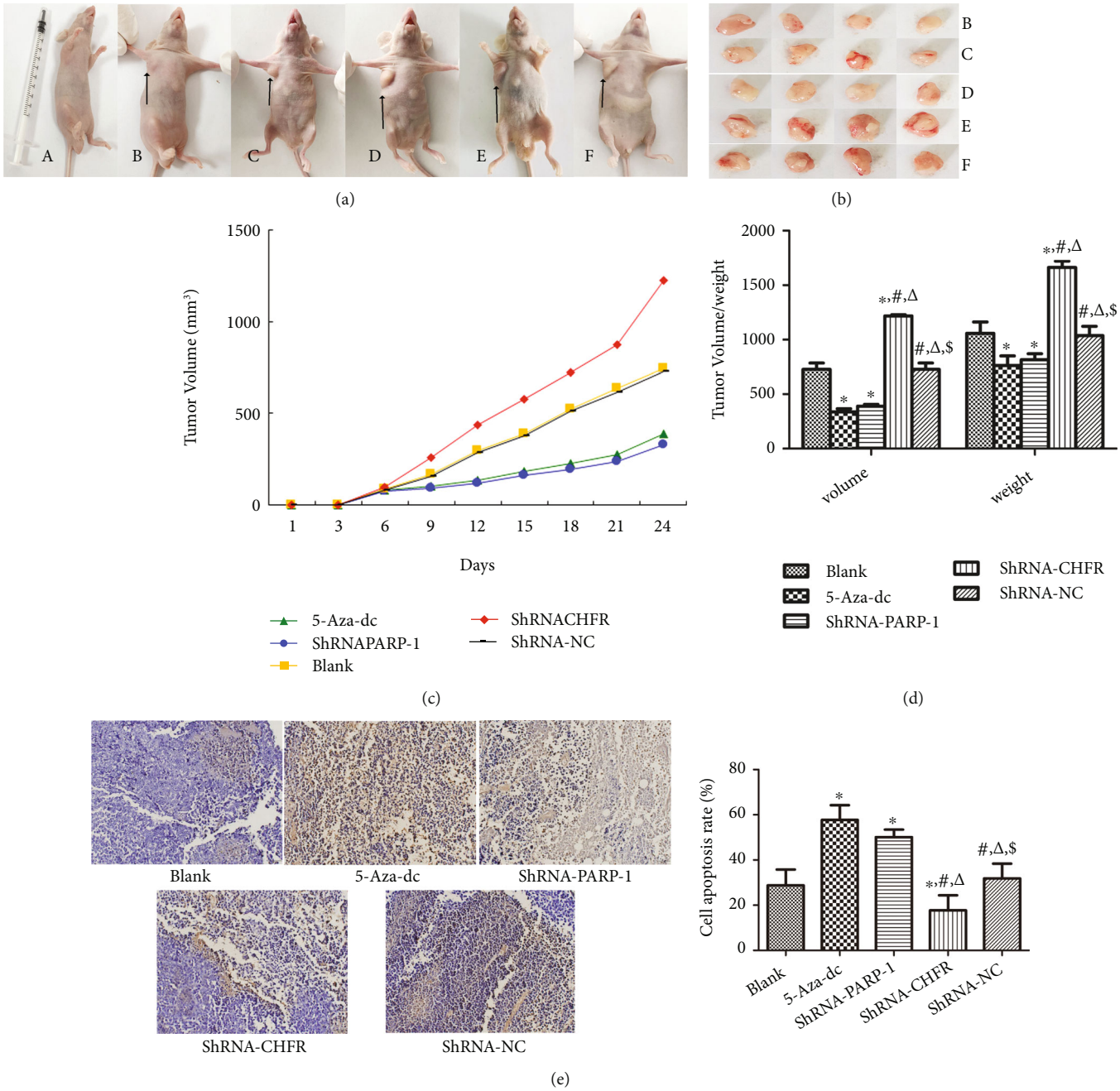

Figure 6: Continued.

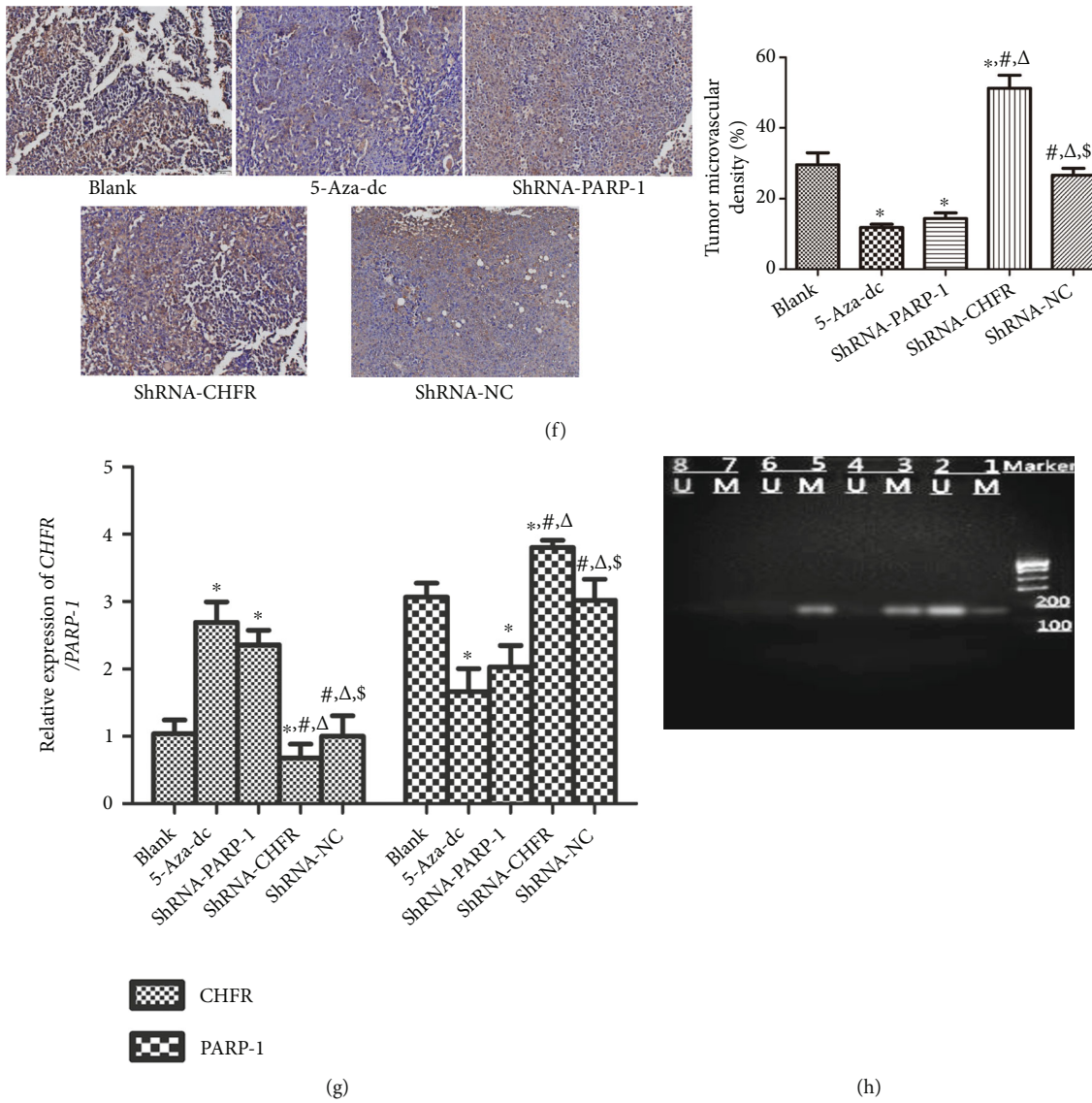

Figure 6: The effects of CHFR and PARP-1 on the tumor xenograft model in vivo. The nude mice were injected with the cell suspension with different treatment for 24 hours. (a) The tumor size in different groups after fed for 24 days. ((A) Normal mice, mice without treatment; (B) 5-Aza-dC group, mice injected with 5-Aza-dc-treated cell suspension; (C) ShRNA-PARP-1 group, mice injected with sh-PARP-1-transfected cell suspension; (D) blank group, mice injected with PBS cell suspension; (E) ShRNA-CHFR group, mice injected with sh-CHFR-transfected cell suspension; and (F) ShRNA-NC group, mice injected with sh-NC-transfected cell suspension). (b) Tumor dissection in each group. (c) Tumor growth curves in the mice of the blank, 5-Aza-dc, ShRNA-PARP-1, ShRNA-CHFR, and ShRNA-NC groups. (d) The tumor volume and weight in the mice of the different groups. (e) Cell apoptosis rate in tumors of the different groups. (f) Tumor microvascular density in the different groups. (g) The mRNA expression levels of *CHFR* and *PARP-1* in the different groups. (h) Determination of methylation of CHFR in mice using MSP (M: methylation; U: Unmethylation; 1, 2: treatment group, the Raji cells-induced mice treated with 5-Aza-Dc; 3, 4: control group, the Raji cells-induced mice with PBS; 5, 6: positive control group, the normal peripheral blood treated with SssI methyl transferase; and 7, 8: blank control group, the normal mice). $^{*}P < 0.05$, compared with the blank group. $^{\#}P < 0.05$, compared with the 5-Aza-dc group. $^{\triangle}P < 0.05$, compared with the ShRNA-PARP-1 group. $^{\$}P < 0.05$, compared with the ShRNA-CHFR group.

of CHFR is not enough to induce apoptosis, whereas on the contrary, it promotes cell transformation and tumorigenesis [44]. In the absence of CHFR, PARP-1 inhibitor is added to capture PARP-1 at the DNA damage sites, and the cellular ability to repair DNA damage may be breached, thus resulting in tumor cell apoptosis [45]. A study of Li et al. [44] also confirmed that CHFR could abolish DNA damage repair, and made gastric tumor cells sensitive to PARP inhibitor therapy. Another study reported that PARP-1 knockdown in the H1299 cells reduced cell migration and colony formation, as well as inhibit the epithelial–mesenchymal transition-related markers, thereby, protecting non-small cell lung cancer [45]. Additionally, Liang et al. found that angiotensin II induced oxidative stress and DNA damage with the increased PARP-1 expression and activity, whereas PARP-1 knockdown by siRNA could reverse the effects

caused by angiotensin II, which suggested that PARP-1 suppression may have protective effects on abdominal aortic aneurysm [46]. Although the mechanisms of PARP-1 knockdown are different from those of PARP-1 inhibitors, we can also conclude that CHFR and PARP-1 might affect Raji cell growth and NHL tumor progression via regulating DNA damage repair. However, the specific relationships between CHFR and PARP-1 in NHL, as well as the roles of CHFR and PARP-1 interaction in DNA damage of NHL Raji cells under different conditions warrant to be further studied.

Aberrant methylation of CHFR was found to be associated with many cancers, and 5-Aza-dC is a DNA-demethylating agent. A previous study [47] reported that 5-Aza-dC treatment decreased trophoblast migration and invasion capacity, and induced mesenchymal to epithelial transition through DNA methylation of epithelial marker genes. Gao et al. showed that CHFR hypermethylation was a frequent event in acute myeloid leukemia, and is independently related to an adverse outcome [48]. Thereout, we hypothesized that CHFR methylation may be associated with NHL, and then determined the CHFR methylation in this study after 5-Aza-dC treatment. We observed that 5-Aza-dC treatment could up-regulate CHFR and down-regulate PARP-1 in Raji cells, and inhibit the tumor growth through the CHFR demethylation *in vitro* and *in vivo*. Methylation is partial methylation, and the occurrence of methylation and demethylation processes is associated with tumorigenesis [49]. The CHFR expression *in vitro* and *in vivo* may be related to the demethylation of some other transcription factors, such as RUNX3 [50], HLTF [51], and RNF8 [52]. Based on our research, we speculated that the existence of CHFR in the cells and tissues might be related to the PARP-1 demethylation, but the specific reasons need to be investigated in the future. Cha et al. [53] indicated that CHFR was expressed in HCT-116 cells, whereas was up-regulated after 5-Aza-dC treatment; as well as combination with 5-Aza-dC suppressed the growth of HCT-116 cells. Our previous study also reported that CHFR was expressed, but lower in the NHL cells and tissues; as well as 5-Aza-dC could eliminate the hypermethylation of CHFR, enhance CHFR expression and cell apoptosis, whereas repress the cell viability of Raji cells [24]. Combined with these findings, it can be inferred that CHFR can be methylated in the lymphoma, and 5-Aza-dC may inhibit tumor formation and Raji cell growth via CHFR demethylation in NHL.

PARP-1 inhibitors have been reported to be used as tumor inhibitors in combination with DNA damaging agents, but few studies have reported the efficacy of PARP-1 knockdown in lymphoma. In this research, we also found that the effects of PARP-1 interference were similar to those of 5-Aza-dC, which imply that PARP-1 knockdown combined with demethylation agents may be more effective for cancer therapy [54, 55]. Our study provides an experimental basis for combined treatment including chemotherapy and demethylation agents. However, the precise mechanisms by which CHFR regulates PARP-1, mitosis, and DNA damage in NHL cells remain unknown, and the roles of 5-Aza-dC in altering the methylation status of other tumor suppressor genes, in addition to CHFR, requires extensive investigation. Furthermore, the roles of PARP-1 in cells and cell biology are more complex, and need to be further explored.

In conclusion, there may be a negative correlation between CHFR and PARP-1 expression in NHL cells under normal conditions, and 5-Aza-dC-treatment may inhibit the growth of NHL cells by regulating CHFR/PARP-1. Additionally, 5-Aza-dC may reduce tumor formation and suppress Raji cell growth via demethylation of CHFR. Our findings will help to improve our understanding of lymphoma therapy, and provide basis for CHFR and PARP-1 as potential therapeutic targets for lymphoma management.

Data Availability

The authors confirm that the data supporting the findings of this study are available within the article.

Ethical Approval

The animal experiments were in line with the ARRIVE guidelines and the animal ethics committee of The Affiliated Hospital of Qingdao University.

Conflicts of Interest

The author(s) declare(s) that they have no conflicts of interest.

Authors' Contributions

Conception and design of the research: Xiao-Dan Liu and Ai-Qin Song; Acquisition of data: Xiao-Dan Liu and Nian-Ju Zheng; Analysis and interpretation of data: Liang Song and Hua Pan; Draft the manuscript: Xiao-Dan Liu and Nian-Ju Zheng; Revision of the manuscript: Hua Pan and Ai-Qin Song. All authors have reviewed and approved the submitted version of the manuscript.

Acknowledgments

This study was supported by Qingdao Municipal Natural Science Foundation (2012-1-3-2-5-nsh), Research Award Fund for Outstanding Middle-aged and Young Scientist of Shandong Province (BS2012YY004), and the Natural Science Foundation of Shandong Province, China (Y2008C170, Q2008C04).

References

[1] J. Bothos, M. K. Summers, M. Venere, D. M. Scolnick, and T. D. Halazonetis, "The Chfr mitotic checkpoint protein functions with Ubc13-Mms2 to form Lys63-linked polyubiquitin chains," *Oncogene*, vol. 22, no. 46, pp. 7101–7107, 2003.

[2] D. M. Scolnick and T. D. Halazonetis, "Chfr defines a mitotic stress checkpoint that delays entry into metaphase," *Nature*, vol. 406, no. 6794, pp. 430–435, 2000.

[3] S. Derks, A. H. Cleven, V. Melotte et al., "Emerging evidence for CHFR as a cancer biomarker: from tumor biology to precision medicine," *Cancer Metastasis Reviews*, vol. 33, no. 1, pp. 161–171, 2014.

[4] T. Fukuda, Y. Kondo, and H. Nakagama, "The anti-proliferative effects of the CHFR depend on the forkhead

associated domain, but not E3 ligase activity mediated by ring finger domain," *PLoS One*, vol. 3, no. 3, article e1776, 2008.

[5] W. Wu, J. Zhao, J. Xiao et al., "CHFR-mediated degradation of RNF126 confers sensitivity to PARP inhibitors in triple-negative breast cancer cells," *Biochemical and Biophysical Research Communications*, vol. 573, pp. 62–68, 2021.

[6] L. Kashima, M. Idogawa, H. Mita et al., "CHFR protein regulates mitotic checkpoint by targeting PARP-1 protein for ubiquitination and degradation," *The Journal of Biological Chemistry*, vol. 287, no. 16, pp. 12975–12984, 2012.

[7] D. Deshmukh and Y. Qiu, "Role of PARP-1 in prostate cancer," *American Journal of Clinical and Experimental Urology*, vol. 3, no. 1, pp. 1–12, 2015.

[8] M. M. Rosado, E. Bennici, F. Novelli, and C. Pioli, "Beyond DNA repair, the immunological role of PARP-1 and its siblings," *Immunology*, vol. 139, no. 4, pp. 428–437, 2013.

[9] K. W. Ryu, D. S. Kim, and W. L. Kraus, "New facets in the regulation of gene expression by ADP-ribosylation and poly(-ADP-ribose) polymerases," *Chemical Reviews*, vol. 115, no. 6, pp. 2453–2481, 2015.

[10] A. J. Smith, S. S. Ball, R. P. Bowater, and I. M. Wormstone, "PARP-1 inhibition influences the oxidative stress response of the human lens," *Redox Biology*, vol. 8, pp. 354–362, 2016.

[11] J. D. Steffen, R. M. Tholey, M. F. Langelier et al., "Targeting PARP-1 allosteric regulation offers therapeutic potential against cancer," *Cancer Research*, vol. 74, no. 1, pp. 31–37, 2014.

[12] J. Yélamos, L. Moreno-Lama, J. Jimeno, and S. O. Ali, "Immunomodulatory roles of PARP-1 and PARP-2: impact on PARP-centered cancer therapies," *Cancers*, vol. 12, no. 2, p. 392, 2020.

[13] W. C. Chung, S. Lee, Y. Kim, J. B. Seo, and M. J. Song, "Kaposi's sarcoma-associated herpesvirus processivity factor (PF-8) recruits cellular E3 ubiquitin ligase CHFR to promote PARP1 degradation and lytic replication," *PLoS Pathogens*, vol. 17, no. 1, p. e1009261, 2021.

[14] Z. Li, H. Zhang, J. Yang, T. Hao, and S. Li, "Promoter hypermethylation of DNA damage response genes in hepatocellular carcinoma," *Cell Biology International*, vol. 36, no. 5, pp. 427–432, 2012.

[15] J. Hoebeeck, E. Michels, F. Pattyn et al., "Aberrant methylation of candidate tumor suppressor genes in neuroblastoma," *Cancer Letters*, vol. 273, no. 2, pp. 336–346, 2009.

[16] A. Tanemura, A. M. Terando, M. S. Sim et al., "CpG island methylator phenotype predicts progression of malignant melanoma," *Clinical Cancer Research*, vol. 15, no. 5, pp. 1801–1807, 2009.

[17] A. Widschwendter, H. M. Muller, H. Fiegl et al., "DNA methylation in serum and tumors of cervical cancer patients," *Clinical Cancer Research*, vol. 10, no. 2, pp. 565–571, 2004.

[18] R. Shanmuganathan, N. B. Basheer, L. Amirthalingam, H. Muthukumar, R. Kaliaperumal, and K. Shanmugam, "Conventional and nanotechniques for DNA methylation profiling," *The Journal of Molecular Diagnostics*, vol. 15, no. 1, pp. 17–26, 2013.

[19] M. Hiraki, Y. Kitajima, S. Sato et al., "Aberrant gene methylation in the peritoneal fluid is a risk factor predicting peritoneal recurrence in gastric cancer," *World Journal of Gastroenterology*, vol. 16, no. 3, pp. 330–338, 2010.

[20] Y. Morioka, K. Hibi, M. Sakai et al., "Aberrant methylation of the CHFR gene in digestive tract cancer," *Anticancer Research*, vol. 26, no. 3A, pp. 1791–1795, 2006.

[21] Z. Sun, J. Liu, H. Jing, S. X. Dong, and J. Wu, "The diagnostic and prognostic value of CHFR hypermethylation in colorectal cancer, a meta-analysis and literature review," *Oncotarget*, vol. 8, no. 51, pp. 89142–89148, 2017.

[22] C. Wang, W. Ma, R. Wei et al., "Clinicopathological significance of CHFR methylation in non-small cell lung cancer: a systematic review and meta-analysis," *Oncotarget*, vol. 8, no. 65, pp. 109732–109739, 2017.

[23] H. Shi, X. Wang, J. Wang, J. Pan, J. Liu, and B. Ye, "Association between CHFR gene hypermethylation and gastric cancer risk: a meta-analysis," *Oncotargets and Therapy*, vol. 9, pp. 7409–7414, 2016.

[24] A. Song, J. Ye, K. Zhang et al., "Aberrant expression of the CHFR prophase checkpoint gene in human B-cell non-Hodgkin lymphoma," *Leukemia Research*, vol. 39, no. 5, pp. 536–543, 2015.

[25] X. Yu, K. Minter-Dykhouse, L. Malureanu et al., "Chfr is required for tumor suppression and Aurora a regulation," *Nature Genetics*, vol. 37, no. 4, pp. 401–406, 2005.

[26] Y. Wang, J. Su, L. Wang et al., "The effects of 5-aza-2′-deoxycytidine and trichostatin a on gene expression and DNA methylation status in cloned bovine blastocysts," *Cellular Reprogramming*, vol. 13, no. 4, pp. 297–306, 2011.

[27] L. Zhou, C. Yang, N. Zhang, X. Zhang, T. Zhao, and J. Yu, "Silencing METTL3 inhibits the proliferation and invasion of osteosarcoma by regulating ATAD2," *Biomedicine & Pharmacotherapy*, vol. 125, p. 109964, 2020.

[28] L. Anjos, A. Z. Loukissas, and D. M. Power, "Proteomics of fish white muscle and western blotting to detect putative allergens," *Methods in Molecular Biology*, vol. 2498, pp. 397–411, 2022.

[29] H. Chehade, A. Fox, G. G. Mor, and A. B. Alvero, "Determination of caspase activation by western blot," *Methods in Molecular Biology*, vol. 2255, pp. 1–12, 2021.

[30] J. Z. Ren and J. R. Huo, "5-aza-2′-deoxycytidine-induced inhibition of CDH13 expression and its inhibitory effect on methylation status in human colon cancer cells in vitro and on growth of xenograft in nude mice," *Zhonghua zhong liu za zhi*, vol. 34, no. 1, pp. 6–10, 2012.

[31] L. M. Privette and E. M. Petty, "CHFR: a novel mitotic checkpoint protein and regulator of tumorigenesis," *Translational Oncology*, vol. 1, no. 2, pp. 57–64, 2008.

[32] Q. Liu, L. Gheorghiu, M. Drumm et al., "PARP-1 inhibition with or without ionizing radiation confers reactive oxygen species-mediated cytotoxicity preferentially to cancer cells with mutant TP53," *Oncogene*, vol. 37, no. 21, pp. 2793–2805, 2018.

[33] N. Martinez-Bosch, M. E. Fernandez-Zapico, P. Navarro, and J. Yelamos, "Poly(ADP-ribose) polymerases: new players in the pathogenesis of exocrine pancreatic diseases," *The American Journal of Pathology*, vol. 186, no. 2, pp. 234–241, 2016.

[34] M. Masutani, H. Nakagama, and T. Sugimura, "Poly-ADP-ribosylation in health and disease," *Cellular and Molecular Life Sciences*, vol. 62, no. 7–8, pp. 769–783, 2005.

[35] L. Wang, W. Cai, W. Zhang et al., "Inhibition of poly(ADP-ribose) polymerase 1 protects against acute myeloid leukemia by suppressing the myeloproliferative leukemia virus oncogene," *Oncotarget*, vol. 6, no. 29, pp. 27490–27504, 2015.

[36] T. Tomoda, T. Kurashige, T. Moriki, H. Yamamoto, S. Fujimoto, and T. Taniguchi, "Enhanced expression of poly (ADP-ribose) synthetase gene in malignant lymphoma," *American Journal of Hematology*, vol. 37, no. 4, pp. 223–227, 1991.

[37] S. R. Shinde, N. R. Gangula, S. Kavela, V. Pandey, and S. Maddika, "TOPK and PTEN participate in CHFR mediated mitotic checkpoint," *Cellular Signalling*, vol. 25, no. 12, pp. 2511–2517, 2013.

[38] C. Wang, W. Xu, J. An et al., "Poly(ADP-ribose) polymerase 1 accelerates vascular calcification by upregulating Runx2," *Nature Communications*, vol. 10, no. 1, p. 1203, 2019.

[39] P. Chang, M. K. Jacobson, and T. J. Mitchison, "Poly(ADP-ribose) is required for spindle assembly and structure," *Nature*, vol. 432, no. 7017, pp. 645–649, 2004.

[40] L. Tentori, A. Muzi, A. S. Dorio et al., "Pharmacological inhibition of poly(ADP-ribose) polymerase (PARP) activity in PARP-1 silenced tumour cells increases chemosensitivity to temozolomide and to a N3-adenine selective methylating agent," *Current Cancer Drug Targets*, vol. 10, no. 4, pp. 368–383, 2010.

[41] J. Wesierska-Gadek, D. Schloffer, M. Gueorguieva, M. Uhl, and A. Skladanowski, "Increased susceptibility of poly(ADP-ribose) polymerase-1 knockout cells to antitumor triazoloacridone C-1305 is associated with permanent G2 cell cycle arrest," *Cancer Research*, vol. 64, no. 13, pp. 4487–4497, 2004.

[42] S. A. Jannetti, G. Carlucci, B. Carney et al., "PARP-1-targeted radiotherapy in mouse models of glioblastoma," *Journal of Nuclear Medicine*, vol. 59, no. 8, pp. 1225–1233, 2018.

[43] M. J. Schiewer, J. F. Goodwin, S. Han et al., "Dual roles of PARP-1 promote cancer growth and progression," *Cancer Discovery*, vol. 2, no. 12, pp. 1134–1149, 2012.

[44] Y. Li, Y. Shi, X. Wang, X. Yu, C. Wu, and S. Ding, "Silencing of CHFR sensitizes gastric carcinoma to PARP inhibitor treatment," *Translational Oncology*, vol. 13, no. 1, pp. 113–121, 2020.

[45] M. Kumar, R. K. Jaiswal, R. Prasad et al., "PARP-1 induces EMT in non-small cell lung carcinoma cells via modulating the transcription factors Smad4, p65 and ZEB1," *Life Sciences*, vol. 269, p. 118994, 2021.

[46] E. S. Liang, W. W. Bai, H. Wang et al., "PARP-1 (poly[ADP-ribose] polymerase 1) inhibition protects from Ang II (angiotensin II)-induced abdominal aortic aneurysm in mice," *Hypertension*, vol. 72, no. 5, pp. 1189–1199, 2018.

[47] Y. Chen, K. Wang, and R. Leach, "5-Aza-dC treatment induces mesenchymal-to-epithelial transition in 1st trimester trophoblast cell line HTR8/SVneo," *Biochemical and Biophysical Research Communications*, vol. 432, no. 1, pp. 116–122, 2013.

[48] L. Gao, F. Liu, H. Zhang, J. Sun, and Y. Ma, "CHFR hypermethylation, a frequent event in acute myeloid leukemia, is independently associated with an adverse outcome," *Genes, Chromosomes & Cancer*, vol. 55, no. 2, pp. 158–168, 2016.

[49] J. Shi, J. Xu, Y. E. Chen et al., "The concurrence of DNA methylation and demethylation is associated with transcription regulation," *Nature Communications*, vol. 12, no. 1, p. 5285, 2021.

[50] S. L. Hu, D. B. Huang, Y. B. Sun et al., "Pathobiologic implications of methylation and expression status of Runx3 and CHFR genes in gastric cancer," *Medical Oncology*, vol. 28, no. 2, pp. 447–454, 2011.

[51] J. M. Kim, E. N. Cho, Y. E. Kwon, S. J. Bae, M. Kim, and J. H. Seol, "CHFR functions as a ubiquitin ligase for HLTF to regulate its stability and functions," *Biochemical and Biophysical Research Communications*, vol. 395, no. 4, pp. 515–520, 2010.

[52] J. Wu, Y. Chen, L. Y. Lu et al., "Chfr and RNF8 synergistically regulate ATM activation," *Nature Structural & Molecular Biology*, vol. 18, no. 7, pp. 761–768, 2011.

[53] Y. Cha, S. Y. Kim, H. Y. Yeo et al., "Association of CHFR promoter methylation with treatment outcomes of irinotecan-based chemotherapy in metastatic colorectal cancer," *Neoplasia*, vol. 21, no. 1, pp. 146–155, 2019.

[54] K. Yuan, Y. Sun, T. Zhou, J. McDonald, and Y. Chen, "PARP-1 regulates resistance of pancreatic cancer to TRAIL therapy," *Clinical Cancer Research*, vol. 19, no. 17, pp. 4750–4759, 2013.

[55] S. Li, Z. Cui, and X. Meng, "Knockdown of PARP-1 inhibits proliferation and ERK signals, increasing drug sensitivity in osteosarcoma U2OS cells," *Oncology Research*, vol. 24, no. 4, pp. 279–286, 2016.